

Aortic Elongation in Bicuspid Aortic Valve with Aortic Stenosis Assessed by Thin-Slice Electrocardiogram-Gated Computed Tomography

Jumpei Fujiwara,¹ MD, Makoto Orii,² MD, Hidenobu Takagi,² MD, Takuya Chiba,³ RT, Tadashi Sasaki,³ RT, Ryoichi Tanaka,⁴ MD, Hajime Kin,⁵ MD, Yoshihiro Morino,¹ MD and Kunihiro Yoshioka,² MD

Summary

Bicuspid aortic valve (BAV) patients with aortic stenosis (AS) are known to develop dilatation of the ascending aorta at a younger age, but the morphology of the aorta in these patients is yet to be investigated. Thus, in this study, we aim to evaluate the aortic morphology of BAV patients with severe AS using thin-slice electrocardiogram (ECG)-gated computed tomography (CT) and identify the possible contributing effect of age.

In this retrospective study, 122 BAV and 154 tricuspid aortic valve (TAV) patients who received aortic valve replacement for severe AS were assessed by thin-slice ECG-gated CT and three-dimensional reconstruction. The morphology of the ascending aorta was also evaluated among BAV patients aged < 70 ($n = 72$) and ≥ 70 ($n = 50$) years old. As per our findings, BAV patients with severe AS had significantly greater diameter ($P < 0.01$), elongation ($P < 0.01$), and tortuosity ($P = 0.03$) of the ascending aorta; minimum aortic arch angle ($P < 0.01$); and significantly lower calcified plaque ($P < 0.01$) compared with those of TAV patients even after adjusting for background. Multiple regression analysis showed that standardized partial regression coefficients (β) of dilatation (0.5) and elongation (0.35) were higher among other measurements of aortic morphology for BAV patients. BAV patients with severe AS aged ≥ 70 years had significantly greater diameter (42.0 [37.2-46.1] mm versus 40.4 [35.2-44.2] mm, $P = 0.049$) and elongation (133.8 [123.5-147.3] mm versus 127.0 [111.0-140.0] mm, $P = 0.01$) of the ascending aorta than those aged < 70 years.

BAV patients with severe AS were determined to have greater dilatation and elongation of the ascending aorta. Moreover, BAV patients older than 70 years had greater diameter and elongation of the ascending aorta.

(Int Heart J 2022; 63: 319-326)

Key words: Thoracic aorta, Aortic morphology, Aortic dilatation, Sievers classification, Arteriosclerosis

The bicuspid aortic valve (BAV) has been identified as the most common congenital cardiac malformation, occurring in 1%-2% of the global population.¹⁾ It is often considered a serious condition with notable valvular risk, particularly of frequent progression to aortic stenosis (AS) requiring aortic valve replacement (AVR).²⁾ BAV with significant AS may also cause frequent and severe aortic complications such as dilatation, aneurysms, and dissection. However, data regarding the degree of aortic dilatation at which the risk of serious aortic events occurs have remained scarce. Thus, there is an urgent clinical need to determine the alternative characteristics of the aorta that would identify BAV patients who could benefit from early interventions to prevent serious aortic events. Recently, thin-slice electrocardiogram (ECG)-gated computed tomography (CT) and three-

dimensional (3D) reconstruction have become the available modalities for a detailed assessment of the aortic morphology.

BAV with significant AS is present in the majority of younger patients compared with tricuspid aortic valve (TAV).³⁾ On the other hand, there are some cases of slow progression of AS, and the proportion of BAV patients with severe AS aged ≥ 70 years was 27%.⁴⁾ However, there have been no data as regards the age-stratified analysis evaluating the aortic morphology of BAV patients with severe AS.

Therefore, in this study, we aim to evaluate the morphology of the ascending aorta and aortic arch using thin-slice ECG-gated CT in BAV patients with severe AS. Age-stratified analysis on aortic morphology in BAV patients with severe AS was also undertaken.

From the ¹Division of Cardiology, Department of Internal Medicine, Iwate Medical University, Yahaba, Japan, ²Department of Radiology, Iwate Medical University, Yahaba, Japan, ³Center for Radiological Science, Iwate Medical University, Yahaba, Japan, ⁴Division of Dental Radiology, Department of Reconstructive Oral and Maxillofacial Surgery, Iwate Medical University, Yahaba, Japan and ⁵Department of Cardiovascular Surgery, Iwate Medical University, Yahaba, Japan.

Address for correspondence: Makoto Orii, MD, Department of Radiology, Iwate Medical University, 2-1-1, Idai-dori, Yahaba, 028-3695, Japan. E-mail: kori931@gmail.com

Received for publication April 18, 2021. Revised and accepted September 27, 2021.

Released in advance online on J-STAGE February 18, 2022.

doi: 10.1536/ihj.21-244

All rights reserved by the International Heart Journal Association.

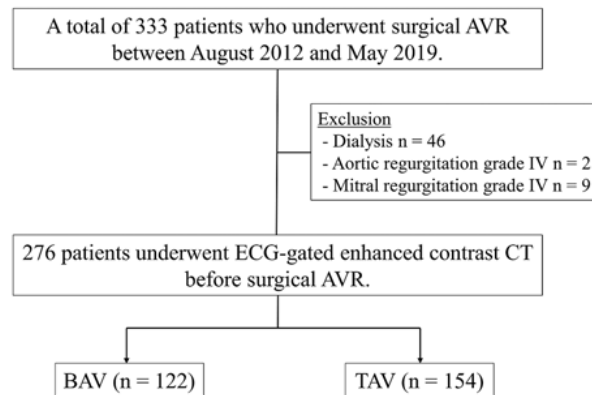


Figure 1. Patient flowchart for the current analysis. AVR, aortic valve replacement; ECG gate, electrocardiogram gate; CT, computed tomography; BAV, bicuspid aortic valve; TAV, tricuspid aortic valve.

Methods

Study population and design: In this retrospective, observational study, 333 consecutive patients with severe AS undergoing thin-slice ECG-gated CT and surgical AVR (SAVR) at Iwate Medical University Hospital from August 2012 to May 2019 were recruited (Figure 1). During the study period, patients underwent SAVR if they had severe AS with an aortic valve area (AVA) $< 1.0 \text{ cm}^2$ or $< 0.6 \text{ cm}^2/\text{m}^2$. We excluded patients who were in dialysis ($n = 46$), with severe aortic regurgitation (AR) ($n = 2$), and with severe mitral regurgitation ($n = 9$). There were no patients with aortic coarctation or right aortic arch. The final study population comprised 276 patients (121 men [44%], mean age 71.3 ± 10.4 years). Board-certified cardiovascular surgeons assessed the presence of BAV ($n = 122$) according to a surgery report. The phenotypes of the aortic valve of BAV patients were classified according to Sievers classification.⁵⁾ The study protocol conforms to the ethical guidelines of the 1975 Declaration of Helsinki as reflected in an a priori approval by the institution's human research committee (MH2019-087) and written informed consent for the data collection was obtained from each patient prior to SAVR.

Echocardiography and standard clinical evaluation: All patients underwent echocardiography before SAVR. All echocardiograms were performed and analyzed by the same operator using an EPIQ 7 ultrasound machine (Philips Healthcare, Inc., Andover, MA). Measurements and recordings were obtained according to the American Society of Echocardiography (ASE) guidelines.⁶⁾ AVA was estimated with quantitative Doppler using the continuity equation. Doppler was used to measure blood flow velocity, pulsed- or color-Doppler or both were used to assess sub-aortic flow and degree of AR, and continuous-wave Doppler was used to measure maximum jet velocity.²⁾ Left ventricular (LV) wall dimensions were estimated from the average of three consecutive two-dimensional images obtained in the parasternal long-axis view according to the ASE's guidelines. The LV ejection fraction was calculated using the biplane modified Simpson's method. Hemoglobin level, estimated glomerular filtration rate (eGFR), uri-

nary protein, and brain natriuretic peptide (BNP) level values were also obtained.

CT image acquisition: Contrast-enhanced CT was performed during breath-holding at end-inspiration using a 320 multi-detector row CT scanner (Aquilion One, Canon Medical Systems, Otawara) before SAVR. The scan protocol consisted of a retrospective ECG-gated helical acquisition from the aortic arch to the cardiac apex. The scan parameters were a slice thickness of $0.5 \text{ mm} \times 80$ rows, pitch factor of 0.140, a gantry rotation speed of 0.275–0.35 s/rotation, a tube voltage of 120 kV, a tube current of 300–450 mA (with the volume EC), and a reconstruction field of view of 200 mm. The reconstruction kernels and levels of iterative reconstruction were FC44 and AIDR 3D standard. Contrast material (iohexol [Omnipaque 350, Daiichi-Sankyo, Tokyo] or iopamidol [Iopamiron 370, Bayer, Osaka]) was administered intravenously at a dose of 450 mg of iodine/kg of body weight with an injection duration of 30 seconds via a 22-gauge peripheral intravenous catheter placed in the right antecubital vein. In all patients, the injection of contrast material was followed by a 30 mL saline flush. The scan start time was controlled by the manual bolus-tracking method with a threshold of 150 HU in the descending aorta. The scan delay after the trigger was 6 seconds because of patient table movement and mechanical delay.⁷⁾

Image analysis: The optimal cardiac phase for evaluating the thoracic aorta was selected using images from 75% of the entire R-R interval. The sources CT angiography data were imported into a workstation (Vitrea, Ver. 7.8, Canon Medical Systems, Otawara). Using the software's vascular package, which includes a "vessel probe" tool, a 3D model of the thoracic aorta with automated removal of bone and soft tissues was generated. An automated centerline was then obtained along the long axis of the aorta between the ostium of the left coronary artery (LCA) and the arch apex with manual correction when required (Figure 2A). In addition to the 3D model, the centerline described by a stretched curved planar reformation (CPR) of the target aorta was also referred (Figure 2B). We defined the centerline length as aortic elongation. A tortuosity index (TI) was calculated on the CPR image as a ratio of the centerline length (mm) of the aorta to the straight-line length (mm) between the two endpoints (Figure 2A). In addition, the largest diameter of the ascending aorta on axial reconstructions perpendicular to the centerline was measured (Figure 2C). The aortic arch angle was measured by starting from the current point, arching along the centerline above and below that point for the cumulative centerline length on both sides (10 mm by default), finding one point on each side, and measuring the angle formed by all three points. The smallest angle was defined as the minimum angle of the aortic arch (Figure 2A).^{8,9)} Calcified plaque volume in the aortic wall and aortic valve was measured as a plaque with CT values ≥ 150 HU. Two reviewers independently performed these measurements, which were then found to be correlated. After confirming a good correlation between the two observers, the mean of the two measurements was obtained to perform the final analyses.

Statistical analysis: All statistical analyses were per-

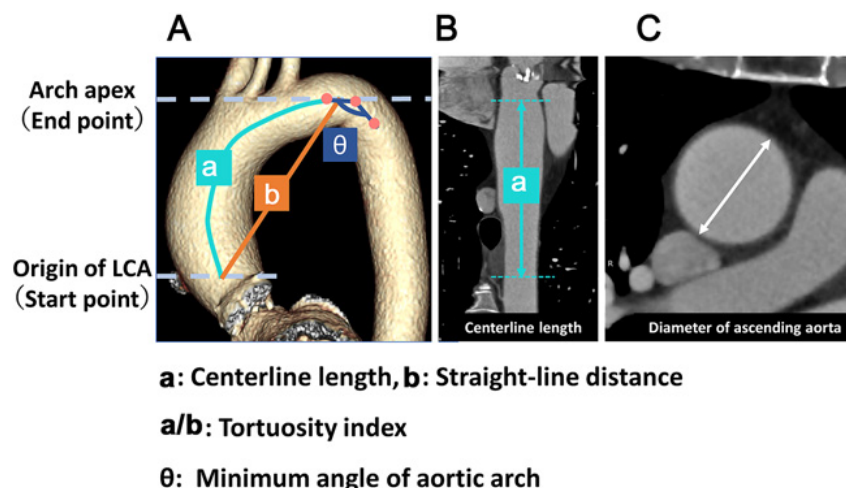


Figure 2. Measurements of aortic geometry. **A:** Three-dimensional model CT image showing thoracic aorta including centerline length (a) and straight-line length (b) between ostium of LCA and arch apex. Tortuosity index is estimated as the ratio of the centerline length of the aorta to the straight-line distance. The smallest angle of the aortic arch was defined as θ . **B:** Stretched curved planar reformat view with the aorta conformed to straight-line including centerline length (aortic elongation) between ostium of LCA and arch apex. **C:** ECG-gated CT scan of MPR. The largest diameter of the ascending aorta on axial reconstructions perpendicular to the centerline was measured. LCA, left coronary artery; CT, computed tomography; MPR, multiplanar reconstruction.

formed using JMP[®] 14.2 (SAS Institute Inc., Cary, NC, USA). Continuous variables are presented as mean \pm SD or median and IQR, whereas categorical variables are expressed as numbers and percentages. Categorical variables were compared using the chi-square test or Fisher's exact test. Continuous variables were compared using the *t*-test or Wilcoxon rank-sum test based on the distribution. We used a simultaneous multiple regression analysis to identify the baseline characteristics including the number of aortic valve leaflets that were independently associated with each CT measurement. Ten control variables, that is, aortic valve leaflets, age, sex, body weight, diabetes, hemoglobin, eGFR, proteinuria, BNP, and LV end-diastolic diameter, were included as independent variables in either CT measurement. We also used multiple regression analyses with 10 unified control variables for analyzing the influence of the number of aortic valve leaflets on the CT measurements. In the multiple regression analyses, the number of aortic valve leaflets, sex, coronary artery disease, diabetes, hypertension, dyslipidemia, chronic kidney disease, proteinuria, and AR were coded as binary value.¹⁰⁾ Pearson correlation coefficients were used to investigate the relationship of each CT measurement in BAV and TAV. Any test with a *P*-value < 0.05 was considered statistically significant.

Results

Population: All 276 patients undergoing SAVR were divided into two groups according to the number of leaflets in aortic valves: BAV group ($n = 122$) and TAV group ($n = 154$) (Figure 1). The baseline clinical characteristics between the two groups are listed in Table I. There were 40 (33%) patients with Sievers type 0 (valve with no raphe), 82 (67%) patients with Sievers type 1 (valve with one ra-

phe), and no patients with Sievers type 2 (valve with two raphe) in BAV. The age of patients in BAV (66.0 ± 10.8 years) was significantly lower than in TAV (75.2 ± 8.0 years, $P < 0.01$) group. Moreover, majority of the patients were male in BAV (60%) group compared to TAV (31%, $P < 0.01$) group. As per our findings, the body surface area was significantly higher in BAV (1.6 ± 0.2 m²) than in TAV (1.5 ± 0.2 m², $P < 0.01$). The proportion of patients with diabetes, hypertension, and chronic kidney disease was found to be significantly lower in BAV than in TAV (17% versus 28%, 47% versus 67%, 29% versus 51%, $P < 0.05$, respectively) group. The hemoglobin and eGFR levels were significantly higher in BAV than in TAV (13.3 ± 1.5 g/dL versus 12.1 ± 1.4 g/dL, 67.8 ± 15.2 mL/minute/1.73 m² versus 61.4 ± 19.3 mL/minute/1.73 m², $P < 0.05$, respectively) group, and serum BNP was significantly lower in BAV (111.5 [58.3-320.3] pg/mL) than in TAV (197.4 [88.1-344.3] pg/mL, $P = 0.01$) group. The LV end-diastolic and end-systolic diameters were significantly higher in BAV than in TAV group (44.0 [41.0-49.0] mm versus 43.0 [39.0-46.0] mm, 27.0 [23.0-33.0] mm versus 25.0 [22.0-29.0] mm, $P < 0.05$, respectively). There were no significant differences between the two groups in terms of LVEF, indexed AVA, and the proportion of AR = 3 (Table I).

Morphology of the ascending aorta and aortic arch in BAV patients with severe AS: Descriptions of the morphology of the ascending aorta and aortic arch in patients with BAV and TAV are listed in Table II. The diameter of the ascending aorta was significantly higher in BAV (40.8 [36.4-45.4] mm) than in TAV (34.9 [32.3-37.0] mm, $P < 0.01$) group. The aortic elongation and TI between the ostium of LCA and the arch apex were also significantly higher in BAV than in TAV (129.5 [119.5-141.3] mm versus 116.5 [105.5-127.3] mm, 1.33 [1.27-1.38] versus 1.30

Table I. Baseline Characteristics

	Total (n = 276)	BAV (n = 122)	TAV (n = 154)	P-value
Age, years	71.3 ± 10.4	66.0 ± 10.8	75.2 ± 8.0	< 0.01
Male patients, n (%)	121 (44)	73 (60)	48 (31)	< 0.01
Height, cm	155.6 ± 9.8	160.0 ± 9.6	152.5 ± 8.9	< 0.01
Weight, kg	56.4 ± 12.0	59.0 ± 11.6	54.4 ± 12.1	< 0.01
BSA, m ²	1.54 ± 0.19	1.60 ± 0.19	1.50 ± 0.19	< 0.01
Comorbidities				
CAD, n (%)	56 (20)	21 (17)	35 (23)	0.24
Diabetes, n (%)	64 (23)	21 (17)	43 (28)	0.03
Hypertension, n (%)	160 (58)	57 (47)	103 (67)	< 0.01
Dyslipidemia, n (%)	121 (44)	48 (49)	73 (47)	0.23
CKD, n (%)	113 (41)	35 (29)	78 (51)	< 0.01
Blood				
Hemoglobin, g/dL	12.6 ± 1.6	13.3 ± 1.5	12.1 ± 1.4	< 0.01
eGFR, mL/minutes/1.73 m ²	64.2 ± 17.9	67.8 ± 15.2	61.4 ± 19.3	0.01
Proteinuria > 0.3 g/Cre, n (%)	24 (9)	8 (7)	16 (10)	0.25
BNP, pg/mL	164.1 [74.3-333.1]	111.5 [58.3-320.3]	197.4 [88.1-344.3]	0.01
Sievers classification in BAV				
Type 0, n (%)		40 (33)		
Type 1, n (%)		82 (67)		
Type 2, n (%)		0 (0)		
Echocardiography				
LVDd, mm	44.0 [40.0-48.0]	44.0 [41.0-49.0]	43.0 [39.0-46.0]	< 0.01
LVDs, mm	26.0 [23.0-31.0]	27.0 [23.0-33.0]	25.0 [22.0-29.0]	0.01
LVEF, %	67.0 [61.0-72.0]	66.0 [60.0-72.0]	68.0 [62.0-72.0]	0.09
AV peak velocity, m/sec	4.90 [4.33-5.35]	4.91 [4.38-5.40]	4.90 [4.28-5.33]	0.39
AV mean PG, mmHg	56.0 [43.0-69.8]	57.0 [47.0-71.0]	54.0 [41.0-68.5]	0.09
AVA index (continuous), cm ² /m ²	0.49 [0.40-0.58]	0.48 [0.40-0.57]	0.51 [0.41-0.61]	0.11
AR = 3, n (%)	25 (9)	9 (7)	16 (10)	0.37

BSA indicates body surface area; CAD, coronary artery disease; CKD, chronic kidney disease; eGFR, estimated glomerular filtration rate; Cre, creatinine; BNP, brain natriuretic peptide; LVDd, left ventricular end-diastolic diameter; LVDs, left ventricular end-systolic diameter; LVEF, left ventricular ejection fraction; AV, aortic valve; AVA, aortic valve area; and AR, aortic regurgitation.

Table II. Morphology of Ascending Aorta and Aortic Arch in Patients with Severe Aortic Stenosis

	Total (n = 276)	BAV (n = 122)	TAV (n = 154)	P-value
Diameter of ascending aorta, mm	36.4 [35.4-41.0]	40.8 [36.4-45.4]	34.9 [32.3-37.0]	< 0.01
Elongation between ostium of LCA and AA, mm	123.0 [108.4-134.0]	129.5 [119.5-141.3]	116.5 [105.5-127.3]	< 0.01
Tortuosity index between ostium of LCA and AA	1.31 [1.27-1.35]	1.33 [1.27-1.38]	1.30 [1.26-1.34]	0.03
Minimum angle of aortic arch, degree	152 [146-156]	150 [142-154]	152 [148-156]	< 0.01
Calcified plaque volume between ostium of LCA and AA, mm ³ /cm ³	36.3 [23.0-55.1]	29.9 [18.0-42.1]	44.5 [30.6-67.7]	< 0.01
Calcified plaque volume of aortic valve, mm ³	4614 [2423-6888]	5599 [2590-8941]	4181 [2351-6054]	< 0.01

LCA indicates left coronary artery; and AA, arch apex.

[1.26-1.34], $P < 0.05$, respectively). The minimum angle of the aortic arch was significantly lower in BAV (150 [142-154] degrees) than that in TAV (152 [148-156] degrees, $P < 0.01$) group. The calcified plaque volume in the aorta's wall was significantly lower in BAV (29.9 [18.0-42.1] mm³/cm³) than that in TAV (44.5 [30.6-67.7] mm³/cm³, $P < 0.01$) group. The calcified plaque volume in the aortic valve was significantly higher in BAV (5599 [2583-9020] mm³) than in TAV (4181 [2351-5973] mm³, $P < 0.01$). In BAV patients, no significant differences were noted in all the measurements of the aorta between the Sievers type 0 and type 1 groups. Figure 3 presents the representative 3D model CT images in BAV and TAV groups.

The results of linear regression analysis based on

BAV are shown in Table III. The single regression analysis showed similar significant differences to the results of the Wilcoxon rank-sum test. The result of simultaneous multiple regression analysis also showed significant differences in all the measurements without the calcified plaque volume in the aortic valve between the two groups ($P < 0.05$, respectively). The results of multiple regression analyses with 10 unified control variables based on BAV are shown in Table IV. The standardized partial regression coefficients (β) of the diameter of the ascending aorta ($\beta = 0.50$) and aortic elongation ($\beta = 0.35$) were higher than other measurements including TI ($\beta = 0.18$). Moreover, the aortic elongation had a good correlation with the diameter of the ascending aorta in TAV (correlation coefficient: $r = 0.54$) and BAV ($r = 0.58$).

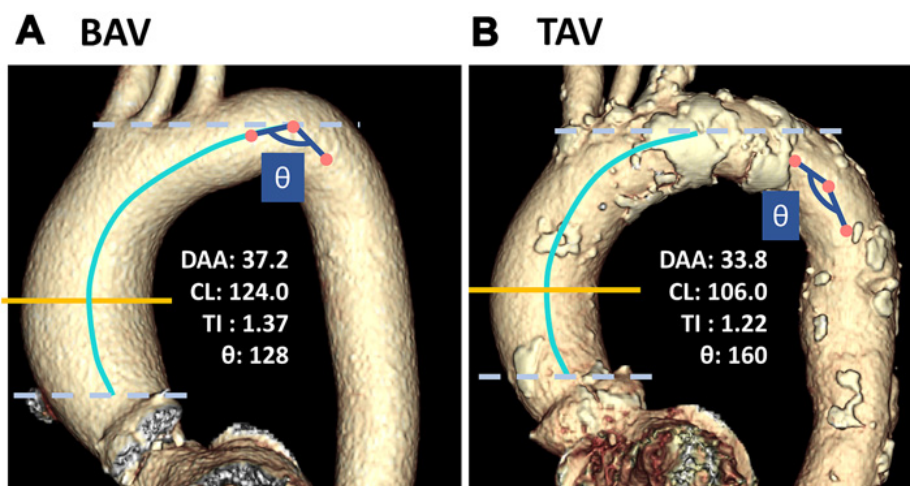


Figure 3. Representative three-dimensional model CT images in BAV and TAV groups. **A:** BAV case. **B:** TAV case. BAV patients with severe AS had greater diameter, elongation, tortuosity index, and lower calcified plaque volume in ascending aorta and acute angle of the aortic arch compared with TAV patients. TI, tortuosity index; θ , the minimum angle of the aortic arch.

Table III. Linear Regression Analysis Based on the BAV

	Single analysis			Multiple regression analysis			
	B	β	P-value	B	β	P-value	r^2
Diameter of ascending aorta, mm	6.2	0.53	< 0.01	6.1	0.51	< 0.01	0.34
Elongation between ostium of LCA and AA, mm	12.1	0.32	< 0.01	13.4	0.36	< 0.01	0.33
Tortuosity index between ostium of LCA and AA	0.022	0.15	0.02	0.02	0.13	0.03	0.09
Minimum angle of aortic arch, degree	-0.031	-0.22	< 0.01	-0.03	-0.21	< 0.01	0.11
Calcified plaque volume between ostium of LCA and AA, mm ³ /cm ³	-0.45	-0.34	< 0.01	-0.3	-0.22	< 0.01	0.28
Calcified plaque volume of aortic valve, mm ³	0.23	0.14	0.02	0.12	0.07	0.26	0.16

LCA indicates left coronary artery; AA, arch apex; B, partial regression coefficient; β , standardized partial regression coefficient; and r^2 , coefficient of determination.

Age-stratified analysis in BAV patients with severe AS:

We then performed subgroup analysis to investigate how age affects the morphology of the ascending aorta and aortic arch in BAV patients with severe AS (Table V). Of the 122 patients with BAV, we divided them into two groups according to age, that is, < 70 years ($n = 72$) and ≥ 70 years old ($n = 50$), in accordance with a past report.⁴⁾ As per our findings, the diameter of the ascending aorta and the aortic elongation was found to be significantly higher in ≥ 70 years compared to that in < 70 years old (42.0 [37.2-46.1] mm versus 40.4 [35.2-44.2] mm, 133.8 [123.5-147.3] mm versus 127.0 [111.0-140.0] mm, $P < 0.05$, respectively). The calcified plaque volume in the aorta's wall was also significantly higher in ≥ 70 years (33.9 [24.3-48.3] mm³/cm³) than in < 70 years old (24.3 [15.4-38.8] mm³/cm³, $P < 0.05$). The aortic elongation had a good correlation with the diameter of the ascending aorta in BAV ≥ 70 years ($r = 0.55$) and BAV < 70 years ($r = 0.60$). On the other hand, no significant differences were noted between the two groups in terms of TI ($P = 0.73$), the minimum angle of the aortic arch ($P = 0.18$), and calcified plaque volume in the aortic valve ($P = 0.14$). Figure 4 shows the representative 3D model CT images in BAV patients aged < 70 years and ≥ 70 years old.

Discussion

To the best of our knowledge, this study is the first to evaluate the aortic morphology of BAV patients with severe AS using thin-slice ECG-gated CT and 3D reconstruction. As per our findings, BAV patients with severe AS had greater diameter, aortic elongation, TI, and lower calcified plaque volume in the ascending aorta and acute angle of the aortic arch compared with TAV patients even after adjusting for background. The standardized partial regression coefficients of the diameter and aortic elongation of ascending aorta were greater than any other measurements including TI. In age-stratified analysis, older BAV patients had significantly greater diameter, elongation, and calcified plaque volume in the ascending aorta than those of the younger age group.

BAV has been described as a disease of the ascending aorta characterized at an early stage by asymptomatic dilatation and later by frequent susceptibility to aneurysm formation and to the most dreaded complication, that is, aortic dissection.²⁾ Furthermore, BAV patients with aneurysms had a faster progression of aortic dilatation in comparison with TAV patients with aneurysms.¹⁾ Thus, prompt resection strategies for the ascending aorta in BAV patients are required to remove diseased tissues at risk of fu-

Table IV. Multiple Regression Analysis with Unified Control Variables Based on the BAV

	Multiple regression analysis			
	B	β	P-value	r^2
Diameter of ascending aorta, mm	5.9	0.50	< 0.01	0.34
Elongation between ostium of LCA and AA, mm	13.2	0.35	< 0.01	0.34
Tortuosity index between ostium of LCA and AA	0.030	0.18	< 0.01	0.11
Minimum angle of aortic arch, degree	-0.029	-0.21	< 0.01	0.12
Calcified plaque volume between ostium of LCA and AA, mm ³ /cm ³	-0.28	-0.21	< 0.01	0.30
Calcified plaque volume of aortic valve, mm ³	0.22	0.14	0.04	0.21

LCA indicates left coronary artery; AA, arch apex; B, partial regression coefficient; β , standardized partial regression coefficient; and r^2 , coefficient of determination.

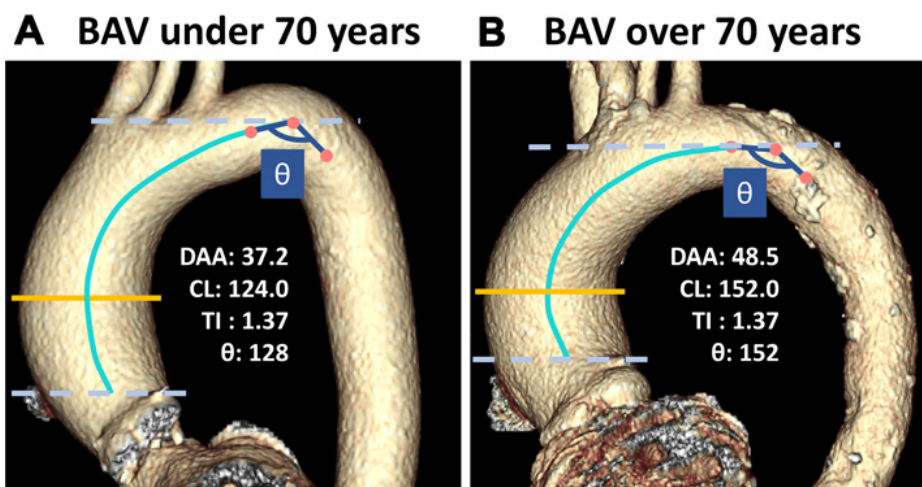


Figure 4. Representative three-dimensional model CT images of BAV patients aged < 70 years and \geq 70 years old. **A:** BAV < 70 years. **B:** BAV \geq 70 years. Older BAV patients had greater diameter and elongation of the ascending aorta and obtuse angle of the aortic arch compared with younger age patients. TI, tortuosity index; θ , the minimum angle of the aortic arch.

ture complications.¹¹⁾

Up till now, the diameter of the ascending aorta has been used to assess the risk of serious aortic events such as aortic dissection in BAV patients. In this study, the BAV group had a greater diameter of the ascending aorta than the TAV group even after adjusting for background. However, there has been no data on the degree of aortic dilatation for risk stratification of serious aortic events in patients with BAV who are undergoing SAVR because of severe AS. Therefore, there is an urgent clinical need to determine the alternative features of the aorta that would identify BAV patients who could benefit from intensive surveillance and early interventions to prevent serious aortic events.

Recently, thin-slice ECG-gated CT and 3D reconstruction have become available, and these advanced imaging techniques are known to provide the accurate morphology of BAV.⁷⁾ In this current study, we evaluated the detailed aortic morphology of BAV patients with severe AS using thin-slice (0.5 mm) ECG-gated CT with 3D reconstruction. On conventional routine chest CT exams without ECG-gating, cardiac motion affects precise delineation of the ascending aorta. CT with ECG-gated reconstruction has made it possible to evaluate the aortic valve and morphology of ascending aorta.^{12,13)} The 3D techniques also allow reproducible aortic measurements at

specific anatomic landmarks and are supplementary to the primary CT images.

Arterial tortuosity has emerged as a reproducible predictor of aortic events in many heritable aortopathies.¹⁴⁻¹⁶⁾ Tortuosity reflects pathologic remodeling in response to progressive structural compromise of the vascular media due to genetic mutations, atherosclerosis, or hemodynamic stress.¹⁴⁾ Therefore, the extent and distribution of tortuosity could be promising indicators of serious aortic events. On the other hand, many measurement methods have been reported for the assessment of tortuosity, but there remain no consensus criteria. Aortic elongation could be assessed simply by the centerline length of the aorta using 3D reconstruction CT compared with any other measurements.^{17,18)} Several studies have revealed the efficacy of the aortic elongation as the marker of serious aortic events.^{19,20)} In BAV patients, aortic elongation, the acute angle of the aortic arch, and lower calcified plaque volume have been reported to correlate with connective tissue disease.^{7,15,21,22)}

In this study, dilatation and elongation of the ascending aorta correlated with BAV than other measurements including tortuosity. The normal aging process is accompanied by gradual aortic dilatation, elongation, higher calcified plaque volume, and obtuse angle of the aortic arch.^{17,18,23)} The results of our study indicate that not only

Table V. Age-Stratified Analysis in BAV Patients with Severe AS

	BAV (n = 122)	< 70 years (n = 72)	≥ 70 years (n = 50)	P-value
Diameter of ascending aorta, mm	40.8 [36.4-45.4]	40.4 [35.2-44.2]	42.0 [37.2-46.1]	0.049
Elongation between ostium of LCA and AA, mm	129.5 [119.5-141.3]	127.0 [111.0-140.0]	133.8 [123.5-147.3]	0.01
Tortuosity index between ostium of LCA and AA	1.33 [1.27-1.38]	1.33 [1.28-1.37]	1.32 [1.27-1.41]	0.73
Minimum angle of aortic arch, degree	150 [142-154]	148 [138-154]	150 [144-154]	0.18
Calcified plaque volume between ostium of LCA and AA, mm ³ /cm ³	29.9 [18.0-42.1]	24.3 [15.4-38.8]	33.9 [24.3-48.3]	0.02
Calcified plaque volume of aortic valve, mm ³	5599 [2590-8941]	5236 [2575-8353]	6330 [2745-9677]	0.14

LCA indicates left coronary artery; and AA, arch apex.

the dilatation of ascending aorta but also aortic elongation might be more progressive in BAV patients with AS. Although several factors must affect the aortic morphology in BAV patients, this study revealed that aortic elongation measured by thin-slice ECG-gated CT and 3D reconstruction is a highly reliable method to evaluate the aortic morphology in daily clinical practice. However, future prospective studies are needed to determine whether aortic elongation can predict longitudinal aortic dilatation and serious aortic events.

Limitations: This study has several limitations. First, this retrospective study of a hospital-based cohort may not accurately represent the natural history of other BAV patients. Second, we did not compare BAV patients with normal controls. All cases with BAV had severe AS, which might have affected the aortic morphology. Third, the rate of BAV patients in this study population was higher than that reported previously.⁴⁾ Recently, severe AS patients with TAV tended to undergo transcatheter aortic valve implantation rather than SAVR. Finally, we used a cross-sectional study design, whereas a longitudinal design would be preferred to investigate the aging process. In addition, we did not compare the same BAV cases in the age-stratified analysis. Therefore, further prospective cohort studies in the same cases of BAV are needed to clarify the relationship between changes in aortic morphology and severe aortic events.

Conclusions

BAV patients with severe AS had more dilated and elongated ascending aorta compared with TAV patients. Moreover, older BAV patients had more dilatation, elongation, and atherosclerotic changes in the ascending aorta than the younger patients with BAV.

Disclosure

Conflicts of interest: None.

Authors' contributions: JF and MO designed and drafted the manuscript. JF, HT, and MO acquired the data and performed the measurements. JF, HT, and HK selected patients with severe AS. HT supported the technical assistance and the statistical analysis. MO, YM, and KY substantially contributed to the manuscript and revised it critically for important intellectual content. All authors approved the submitted version.

References

1. Michelena HI, Prakash SK, Della Corte A, *et al.* Bicuspid aortic valve: identifying knowledge gaps and rising to the challenge from the International Bicuspid Aortic Valve Consortium (BAVCon). *Circulation* 2014; 129: 2691-704.
2. Michelena HI, Desjardins VA, Avierinos JF, *et al.* Natural history of asymptomatic patients with normally functioning or minimally dysfunctional bicuspid aortic valve in the community. *Circulation* 2008; 117: 2776-84.
3. Fedak PW, Verma S, David TE, Leask RL, Weisel RD, Butany J. Clinical and pathophysiological implications of a bicuspid aortic valve. *Circulation* 2002; 106: 900-4.
4. Passik CS, Ackermann DM, Pluth JR, Edwards WD. Temporal changes in the causes of aortic stenosis: a surgical pathologic study of 646 cases. *Mayo Clin Proc* 1987; 62: 119-23.
5. Sievers HH, Schmidtke C. A classification system for the bicuspid aortic valve from 304 surgical specimens. *J Thorac Cardiovasc Surg* 2007; 133: 1226-33.
6. Lang RM, Bierig M, Devereux RB, *et al.* Recommendations for chamber quantification: a report from the American Society of Echocardiography's Guidelines and Standards Committee and the Chamber Quantification Writing Group, developed in conjunction with the European Association of Echocardiography, a branch of the European Society of Cardiology. *J Am Soc Echocardiogr* 2005; 18: 1440-63.
7. Tanaka R, Yoshioka K, Niinuma H, Ohsawa S, Okabayashi H, Ehara S. Diagnostic value of cardiac CT in the evaluation of bicuspid aortic stenosis: comparison with echocardiography and operative findings. *AJR Am J Roentgenol* 2010; 195: 895-9.
8. Choudhry FA, Grantham JT, Rai AT, Hogg JP. Vascular geometry of the extracranial carotid arteries: an analysis of length, diameter, and tortuosity. *J Neurointerv Surg* 2016; 8: 536-40.
9. d'ostrevy N, Ardellier FD, Cassagnes L, *et al.* The apex of the aortic arch backshifts with aging. *Surg Radiol Anat* 2017; 39: 703-10.
10. Akazawa N, Harada K, Okawa N, Tamura K, Moriyama H. Low body mass index negatively affects muscle mass and intramuscular fat of chronic stroke survivors. *PLoS One* 2019; 14: e0211145.
11. Guzzardi DG, Barker AJ, van Ooij P, *et al.* Valve-related hemodynamics mediate human bicuspid aortopathy. *J Am Coll Cardiol* 2015; 66: 892-900.
12. Lu TL, Huber CH, Rizzo E, Dehmshki J, von Segesser LK, Qanadli SD. Ascending aorta measurements as assessed by ECG-gated multi-detector computed tomography: a pilot study to establish normative values for transcatheter therapies. *Eur Radiol* 2009; 19: 664-9.
13. Fallenberg M, Juergens KU, Wichter T, Scheld HH, Fischbach R. Coronary artery aneurysm and type-A aortic dissection demonstrated by retrospectively ECG-gated multislice spiral CT. *Eur Radiol* 2002; 12: 201-4.
14. Alhafez BA, Truong VTT, Ocasionoz D, *et al.* Aortic arch tortuosity, a novel biomarker for thoracic aortic disease, is increased in adults with bicuspid aortic valve. *Int J Cardiol* 2019; 284: 84-9.

15. Han HC. Twisted blood vessels: symptoms, etiology and biomechanical mechanisms. *J Vasc Res* 2012; 49: 185-97.
16. Shirali AS, Bischoff MS, Lin HM, *et al.* Predicting the risk for acute type B aortic dissection in hypertensive patients using anatomic variables. *JACC Cardiovasc Imaging* 2013; 6: 349-57.
17. Adriaans BP, Heuts S, Gerretsen S, *et al.* Aortic elongation part I: the normal aortic ageing process. *Heart* 2018; 104: 1772-7.
18. Sugawara J, Hayashi K, Yokoi T, Tanaka H. Age-associated elongation of the ascending aorta in adults. *JACC Cardiovasc Imaging* 2008; 1: 739-48.
19. Heuts S, Adriaans BP, Gerretsen S, *et al.* Aortic elongation part II: the risk of acute type A aortic dissection. *Heart* 2018; 104: 1778-82.
20. Krüger T, Forkavets O, Veseli K, *et al.* Ascending aortic elongation and the risk of dissection. *Eur J Cardiothorac Surg* 2016; 50: 241-7.
21. Ho VB, Bakalov VK, Cooley M, *et al.* Major vascular anomalies in Turner syndrome: prevalence and magnetic resonance angiographic features. *Circulation* 2004; 110: 1694-700.
22. Kim HK, Gottliebson W, Hor K, *et al.* Cardiovascular anomalies in Turner syndrome: spectrum, prevalence, and cardiac MRI findings in a pediatric and young adult population. *AJR Am J Roentgenol* 2011; 196: 454-60.
23. Davies RR, Kaple RK, Mandapati D, *et al.* Natural history of ascending aortic aneurysms in the setting of an unreplaced bicuspid aortic valve. *Ann Thorac Surg* 2007; 83: 1338-44.